Development of Three-Dimensional Whole-Body Musculoskeletal Model for Various Motion Analyses*

Kazunori HASE** and Nobutoshi YAMAZAKI***

A simulation model for biomechanical analysis was developed in order to calculate the internal loads, such as muscular tension and energy consumption, from measured kinesiological data for various kinds of motion. In this model, the human body is divided into a maximum of nineteen rigid segments connected to each other with ball joints. A maximum of 156 skeletal muscles throughout the body are modeled as tensile force generators which include physiological elements that consume mechanical energy. The component ratio among muscle fiber types, number of body segments and number of degrees of joint freedom can be changed easily, and according to the alteration of the segment number, the musculoskeletal system is changed automatically. This flexibility is of benefit in application of the method to various motion analyses. Three-dimensional bipedal walking was analyzed using a simplified model, and rowing motions were analyzed using the whole-body model.

Key Words: Biomechanics, Human Engineering, Muscle and Skeleton, Muscular Tension, Metabolic Energy

1. Introduction

Biomechanical analysis of human motion using a musculoskeletal model has been widely applied in fields including ergonomics, sports science, and rehabilitation engineering[1),(2)]. The model analysis method can be used to calculate the internal loads such as forces on bones, tensions of muscles and ligaments, and energy consumption from measured data. In contrast to the usefulness and wide-ranging applicability of this method, however, development of an appropriate model is difficult and requires knowledge of not only dynamics but also anatomy and physiology. Therefore most models which have been developed are very simple in structure, and their applications are limited to some specific body motions.

In this study, we developed a three-dimensional whole-body musculoskeletal model, which can be modified easily according to the purpose of various motion analyses. This model is expected to become a convenient tool in biomechanics.

2. Whole Body Model and Its Calculation Method

The following three models are necessary for calculation of the internal loads: a rigid link model for calculation of joint torques from measured joint displacements and external forces acting on the body segments, a musculoskeletal model for calculation of muscle tensions from the calculated joint torques, and a muscle model for calculation of energy consumption from the calculated muscle tensions.

2.1 Rigid link model and calculation of joint torques

As shown in Fig. 1(a), the mass distribution of the whole body was approximated as a three-dimensional rigid link system that consists of 19 segments: 4 segments of each leg, 3 segments of each arm, 3

* Received 13th June, 1996. Japanese original: Trans. Jpn. Soc. Mech. Eng., Vol. 61, No. 591, C (1995), pp. 4417-4422 (Received 3rd April, 1995)

** Institute of Biomedical Engineering, Graduate School of Science and Technology, Keio University, 3-14-1 Hiyoshi, Kohoku-ku, Yokohama, Kanagawa 223, Japan

*** Department of Mechanical Engineering, Faculty of Science and Technology, Keio University, 3-14-1 Hiyoshi, Kohoku-ku, Yokohama, Kanagawa 223, Japan

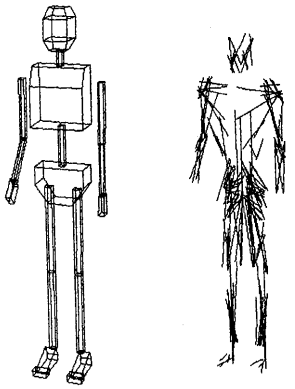

(a) Rigid link model (b) Musculoskeletal model

Fig. 1 Mechanical model of whole body

segments of the trunk, and 2 segments corresponding to the neck and head. All joints were assumed to be ball joints. Additionally, in the leg joints, the following passive torque[3] exerted by resistive elements around the joint was considered:

$$n^p = k_1 \exp\{-k_2(\phi - k_3)\} - k_4 \exp\{-k_5(k_6 - \phi)\} - c\dot{\phi}, \quad (1)$$

where n^p is the resistive torque exerted by ligaments and the capsule of the joint, ϕ is the joint angle, and k_i and c are coefficients. The resistive torque acts independently around each joint axis.

The elastic (k_i) and viscous (c) coefficients in Eq.(1) are listed in Table 1. These values were mainly obtained from the literature[3], but the viscous coefficient of knee joint was modified by referring to Sasada et al.[4] The physical parameters such as mass and moment of inertia of each segment were estimated using the multiple regression equations of stature and body weight given by Chandler et al.[5] and Zatsiorsky and Seluyanov[6]. The body segments in these literature were redivided so as to be able to use them for our link model.

In regard to this rigid link model, the joint reaction force $\boldsymbol{f}_i^J$ on the ith link is given by

$$\boldsymbol{f}_i^J = \boldsymbol{f}_{i-1}^J + m_i \ddot{\boldsymbol{r}}_i^G - \sum_k \boldsymbol{f}_{ik}^E - m_i \boldsymbol{g}, \quad (2)$$

and the joint torque $\boldsymbol{n}_i^J$ is given by

$$\begin{aligned}\boldsymbol{n}_i^J = {} & \boldsymbol{n}_{i-1}^J + \boldsymbol{T}_i\{{}^i\boldsymbol{I}_i\,{}^i\dot{\boldsymbol{\omega}}_i + {}^i\boldsymbol{\omega}_i \times ({}^i\boldsymbol{I}_i\,{}^i\boldsymbol{\omega}_i) + {}^i\boldsymbol{n}_i^P\} \\ & - \boldsymbol{T}_{i-1}{}^{i-1}\boldsymbol{n}_{i-1}^P \\ & - (\boldsymbol{r}_i^J - \boldsymbol{r}_i^G) \times \boldsymbol{f}_i^J + (\boldsymbol{r}_{i-1}^J - \boldsymbol{r}_i^G) \times \boldsymbol{f}_{i-1}^J \\ & - \sum_k \{(\boldsymbol{r}_{ik}^E - \boldsymbol{r}_i^G) \times \boldsymbol{f}_{ik}^E + \boldsymbol{n}_{ik}^E\}, \end{aligned} \quad (3)$$

where $\boldsymbol{f}_{ik}^E$ is the kth external force, $\boldsymbol{g}$ is the acceleration of gravity, $\boldsymbol{T}_i$ is the rotational matrix (3×3) from the relative coordinate system on each segment to the absolute coordinate system, ${}^i\boldsymbol{\omega}_i$ is the angular velocity vector, ${}^i\boldsymbol{n}_i^P$ is the resistive torque of the passive element at the joint, $\boldsymbol{r}_i^J$ is the position vector of the center of the joint, $\boldsymbol{r}_i^G$ is the position vector of the center of gravity of the segment, $\boldsymbol{r}_{ik}^E$ is the position vector of application of the external force, $\boldsymbol{n}_{ik}^E$ is the external torque, m_i is the segment mass, and ${}^i\boldsymbol{I}_i$ is the moment-of-inertia tensor of each segment. The left superscripts, i and $i-1$, indicate that the vector and tensor are described in the relative coordinate systems on each segment. The parameters without left superscripts are expressed in the absolute coordinate system. The meaning of the superscripts is the same in the following expressions.

Table 1 Coefficients of passive element function at joints

	Ankle	Knee	Hip
k_1[Nm]	2.0	3.1	2.6
k_2[1/rad]	5.0	5.9	5.8
k_3[rad]	0.52	-1.92	-0.52
k_4[Nm]	9.0	10.5	8.7
k_5[1/rad]	5.0	11.8	1.3
k_6[rad]	1.92	0.10	1.92
c [Nms/rad]	0.943	1.72	1.09

All positions and external forces in Eq.(2) and all angles and external torques in Eq.(3) were obtained from measurements of actual motion. Mass and moment of inertia can also be calculated using the rigid link model. Consequently, by solving recurrently the inverse dynamic problem as an open chain link system, all joint reaction forces and all joint torques can be obtained from the terminal segments such as feet, hands and head to the upper trunk segment. Because measured data are generally expressed in the absolute coordinate system, the calculation was done in the absolute coordinate system.

2.2 Musculoskeletal model

Because of the complexity of the anatomical structure, the musculoskeletal model has been made as simple as possible within the limits of the purpose of analysis[7],[8]. In this study, we attempted to develop a detailed model which can be used in various motion analyses. The constructed musculoskeletal model includes 44 muscles per leg, 20 muscles per arm, 16 muscles of the trunk, and 12 muscles of the neck as shown in Fig. 1(b). Thus, the total number of whole-body muscles is 156. The lines shown in Fig. 1(b) represent the modeled muscles. The muscular tension was assumed to generally act through a straight line from the origin to the insertion of each muscle. In the case that the direction of the muscle changes considerably, several intermediate "via points" were inserted on the line.

Lever arm ${}^i\boldsymbol{r}_{im}^M$ and the length L_m^{MT} of the mth muscle are given by

$${}^i\boldsymbol{r}_{im}^M = {}^i\boldsymbol{l}_{im}^p \times {}^i\boldsymbol{f}_{im}^M, \quad (4)$$

$${}^i\boldsymbol{f}_{im}^M = \frac{{}^i\boldsymbol{l}_{im}^p - {}^i\boldsymbol{l}_{im}^{p+1}}{|{}^i\boldsymbol{l}_{im}^p - {}^i\boldsymbol{l}_{im}^{p+1}|}, \quad (5)$$

$$L_m^{MT} = \sum_p |{}^i\boldsymbol{l}_{im}^p - {}^i\boldsymbol{l}_{im}^{p+1}|, \quad (6)$$

Table 2 Examples of coordinates of muscle lines

Muscle	Coordinate system	x	y	z
Tibialis anterior	Calf	.042	-.032	.832
	Foot	.111	.111	.811
	Foot	-.089	.222	.489
Soleus	Calf	-.116	.000	.874
	Foot	-.289	.000	1.289
Vastus medialis	Thigh	-.036	-.018	.636
	Thigh	.118	.000	.136
	Thigh	.118	.000	.027
	Calf	.084	.000	.937
Biceps femoris, L	Hip	-.750	-.750	-.125
	Calf	-.116	-.084	.937
Rectus femoris	Hip	.542	-1.375	.125
	Thigh	.118	.000	.136
	Thigh	.118	.000	.027
	Calf	.084	.000	.937
Iliacus	Hip	.708	-1.125	.708
	Hip	.667	-1.125	-.292
	Thigh	-.036	-.027	.755
Adductor longus	Hip	.500	-.167	-.542
	Thigh	-.027	-.009	.418
Gluteus medius	Hip	-.708	-.708	-.750
	Thigh	-.027	.000	.418
Gluteus maximus	Hip	-1.083	-.375	.167
	Hip	-1.167	-1.042	-.292
	Thigh	-.091	-.118	.718

where ${}^{i}\boldsymbol{l}_{im}^{p}$ is the pth via point vector of the mth muscle with respect to ith joint expressed in the ith segment coordinate system, and ${}^{i}\boldsymbol{f}_{im}^{M}$ is the cosine vector of the muscle line. The coordinates of the origin, insertion, and via point were mainly obtained from the literature[9]. The data which are not on the literature, were measured from an anatomical chart[10]. As an example of the coordinates, those of principal muscles of the modeled leg are shown in Table 2. Each coordinate is normalized by the corresponding segment length. The origin of the coordinate system is defined as the distal joint point, the z axis coincides with the longitudinal axis of the segment, the y axis is selected as the rotational axis of the joint, and the x axis is defined as the outer product of the y and z axis vector.

2.3 Simplification of the whole-body model

The number of segments in the standard model is easily changed by removing the segments unnecessary for the purpose of analysis. In this simplification, the segment mass m, the position of the center of gravity $\boldsymbol{r}^{G}$, and the moment-of-inertia tensor $\boldsymbol{I}$ are remodeled as follows:

$$m_{i'}=\sum_{i}\delta_{i}^{i'}m_{i}, \tag{7}$$

$${}^{i'}\boldsymbol{r}_{i'}^{G}=\frac{\sum_{i}\delta_{i}^{i'}m_{i}({}^{i'}\boldsymbol{T}_{i}^{i}\boldsymbol{r}_{i}^{G}+{}^{i'}\boldsymbol{r}_{i}^{O})}{\sum_{i}\delta_{i}^{i'}m_{i}}, \tag{8}$$

$$I_{di'}=\sum_{i}\delta_{i}^{i'}\left[I_{di}+m_{i}\{(p_{d'})^{2}+(p_{d''})^{2}\}\right], \tag{9}$$

$$(p_{x},p_{y},p_{z})^{T}=\{{}^{i'}\boldsymbol{T}_{i}^{i}\boldsymbol{r}_{i}^{G}+{}^{i'}\boldsymbol{r}_{i}^{O}\}-{}^{i'}\boldsymbol{r}_{i'}^{G}$$

$$\begin{cases} d'=y,\ d''=z & \text{for } d=x \\ d'=z,\ d''=x & \text{for } d=y \\ d'=x,\ d''=y & \text{for } d=z \end{cases}$$

where i is the segment number of the standard model, i' is the segment number of the simplified model, and $\delta_{i}^{i'}$ is equal to 1 if the ith segment is included in the i'th segment and is equal to 0 otherwise. The eliminated segments are generally combined with the adjacent proximal segment. However, if the head segment is removed, it is combined with the upper trunk. ${}^{i'}\boldsymbol{T}_{i}$ is the rotational matrix from the relative coordinate system of the ith segment to the relative coordinate system of the i'th segment, and ${}^{i'}\boldsymbol{r}_{i}^{O}$ is the position vector of the origin of the relative coordinate system of the ith segment that is expressed in the relative coordinate system of the i'th segment.

These values of the standard model were determined assuming a standing posture. The moment-of-inertia tensor in the simplified model can be calculated by simply added the principal moment of inertia $I_{d}(d=x,y,z)$ of the standard model using a theorem of parallel axes. In Eq.(9), $p_{d}(d=x,y,z)$ is the relative distance of the center of gravity between the i'th segment and the ith segment. The resistive torque exerted by passive elements of each joint is assumed to be the same even if segments are combined. The degree of freedom in segment motion can also be reduced for application of two-dimensional analysis.

The musculoskeletal model is automatically simplified according to the modification of the rigid link model. If a segment is eliminated, the muscles connected to the segment are also eliminated from the musculoskeletal model. The reduction of the number of degrees of freedom in the musculoskeletal model is performed by projecting the three-dimensional coordinates of arrangements of muscles on the restricted plane.

2.4 Muscle model

After the Hill's two-element model, various kinds of complicated muscle model were proposed[7),(11),(12)]. In this study, referring to reports by Pierrynowsky and Morrison[7] and Hatze[11], we adopted the four-element muscle model shown in Fig. 2. This model consists of a contractile element CE, a series elastic element SE, a parallel elastic element PE, and a tendon element T. In each contractile element, the type of muscle fiber (slow-oxidative: SO, first-oxidative: FO, first-glycolytic: FG) and the pennate angle can be changed easily. The superscripts M and MT denote respectively the variables of a muscle without tendons and the variables of a total muscle including tendons.

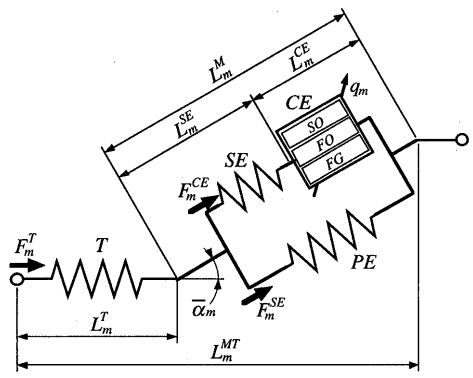

Fig. 2 Muscle model

The normalized muscle active state q_m was chosen as the control variable from the nervous system to the mth muscle, and the following equations were derived.

$$q_{SOm}=q_m,$$
$$q_{FOm}=q_m^{1.54},$$
$$q_{FGm}=q_m^{1.54}, \tag{10}$$

where $q_{nm}(n=SO, FO, FG)$ is the active state of each fiber type in the muscle. These equations were derived from the model of muscle fatigue presented by Dul et al.[13]

The force exerted by each muscle fiber F_{nm}^{CE} is given by

$$F_{nm}^{CE}=\bar{F}_{nm}^{CE}k(\xi_m)h_n(\dot{\eta}_m, \xi_m)q_{nm}, \tag{11}$$

where $\bar{F}_{nm}^{CE}$ is the maximum isometric force exerted by each muscle fiber, $k(\xi_m)$ is the force-length relationship, and $h_n(\dot{\eta}_m, \xi_m)$ is the force-velocity relationship of the muscle contractile element. These relationships are expressed as follows[11]:

$$k(\xi_m)=0.32+0.71\exp\{-1.112(\xi_m-1)\}\times\sin\{3.722(\xi_m-0.656)\}, \tag{12}$$
$$h_n(\dot{\eta}_m, \xi_m)=\{1+\tanh(a_{1n}\dot{\eta}_m)\}/a_{2n}-a_{3n}\exp\{-2.6(\xi_m-1)\}, \tag{13}$$

where ξ_m is the length of the contractile element normalized by the natural length of the contractile element $\bar{L}_m^{CE}$ (i.e., $\xi_m=L_m^{CE}/\bar{L}_m^{CE}$) and $\dot{\eta}_m$ is the contractile velocity normalized by the maximum contractile velocity $\bar{L}_m^{CE}$ (i.e., $\dot{\eta}_m=\dot{L}_m^{CE}/\bar{L}_m^{CE}$; negative for contraction). The maximum contractile velocity $\bar{L}_m^{CE}$ is assumed as a constant value (3.0 [m/sec]). Coefficient a_{1n} is 3.30, 2.55 and 2.55 where $n=SO, FO, FG$, respectively. In the same order, $a_{2n}=0.997$, 0.988, 0.988; and $a_{3n}=0.00272$, 0.0123, 0.0123.

The force exerted by the contractile element F_m^{CE} is obtained as the sum of the forces exerted by each muscle fiber described above:

$$F_m^{CE}=\sum_{n=1}^{3}F_{nm}^{CE}. \tag{14}$$

The force exerted by the parallel elastic element F_m^{PE} is expressed as follows[11]:

$$F_m^{PE}=0.00159\,\bar{F}_m^{CE}[\exp\{5.40(L_m^M-\bar{L}_m^M)/\bar{L}_m^M\}-1],$$
$$\bar{F}_m^{CE}=\sum_{n=1}^{3}\bar{F}_{nm}^{CE}, \tag{15}$$

where L_m^M is the length of the muscle fiber and $\bar{L}_m^M$ is the natural fiber length.

The muscular tension F_m^T is finally calculated as

$$F_m^T=(F_m^{CE}+F_m^{PE})\cos\bar{\alpha}_m, \tag{16}$$

where $\bar{\alpha}_m$ is the given pennate angle. Consequently, if the length of the contractile element L_m^{CE}, the length of the muscle fiber L_m^M, and the contractile velocity $\dot{L}_m^{CE}$ are known, the muscular tension F_m^T can be calculated using Eqs. (10) to (16).

In these calculations, the geometrical variables such as the lengths L_m^{CE} and L_m^M, and the velocity $\dot{L}_m^{CE}$ were assumed to be constant values, but they actually change with the tension of the muscle itself. For this reason, these geometrical variables were recalculated after the above-mentioned estimation of muscular tension. The calculation algorithm will be explained in the next section. If the muscular tension F_m^T and the force exerted by the contractile element F_m^{CE} have already been calculated, the geometrical relationships of muscles are given by the following equations:

$$L_m^M=\bar{L}_m^M+(\Delta L_m^{MT}-\Delta L_m^T)/\cos\bar{\alpha}_m, \tag{17}$$

where L_m^M is the length of the muscle fiber. In Eq. (17), the pennate angle $\bar{\alpha}_m$ is assumed to be independent of the muscular contraction. ΔL_m^{MT} is the total change in the length of the total muscle elements and tendon calculated using Eq. (6). ΔL_m^T defined by Eq. (18) is the change in the length of the tendon taken from the tendon stress-strain curve derived by Benedict et al.[14]

$$\Delta L_m^T=L_m^T-\bar{L}_m^T=\frac{\bar{L}_m^T F_m^T}{1400\,\bar{A}_m^T}, \tag{18}$$

where $\bar{L}_m^T$ is the tendon length, and $\bar{A}_m^T$ is the cross-sectional area of the tendon.

The length of a series elastic element L_m^{SE} is expressed as follows[7]:

$$L_m^{SE}=\bar{L}_m^{SE}+\bar{L}_m^M(0.21188\,\zeta_m-0.22625\,\zeta_m^2+0.08438\,\zeta_m^3),$$
$$\zeta_m=F_m^{CE}/\bar{F}_m^{CE}, \tag{19}$$

where $\bar{L}_m^{SE}$ is the natural length of a series elastic element L_m^{SE}.

The length of a contractile element L_m^{CE} is given by

$$L_m^{CE}=L_m^M-L_m^{SE}. \tag{20}$$

The contraction velocity of the contractile element $\dot{L}_m^{CE}$ is obtained by numerical differentiation of the length of the contractile element L_m^{CE}.

2.5 Calculation of muscular tension

The joint torque calculated using Eq. (3) must be exerted by muscle activities. On the other hand, the muscular torque at a joint, which should be balanced to the calculated joint torque, is defined as the sum of

the product of each muscular tension around the joint (Eq.(16)) and its lever arm (Eq.(4)). However, the number of equilibrium equations of the joint torque and muscular torque is equal to only the number of total degrees of freedom of joints, and it is too small for solving the unknown muscular tensions. In order to solve the problem, various kinds of optimization technique were proposed[15] based on some objective functions for muscle activity. In this study, we adopted the summation of endurance times of muscle tensions proposed by Dul et al.[13] and modified it for dynamic activities. The endurance time T_m [sec] represents the durability of constant muscular tension, and is given by

$$T_m=b_1(100\ q_m)^{b2},$$
$$b_1=\exp(3.48+0.169\ R_{som}),$$
$$b_2=-0.25-0.036\ R_{som}. \tag{21}$$

Equations (21) are the functions of the component ratio of the slow muscle fiber R_{som} [%] and the active state q_m of the muscle.

Muscular tensions are calculated so as to maximize the sum of the endurance times of each muscle as shown in Eq.(22). This means minimization of muscular fatigue.

$$J=\sum_m T_m\rightarrow\max \tag{22}$$

Actually, muscular tensions are obtained by solving the following nonlinear optimization problem.

Variables: q_m

Objective function: $J'=\sum_m 1/T_m\rightarrow\min$ (23)

Constraints:

$F_m^T=F_m^T(q_m)$ (10)-(16)

$F_m^T\geq 0$ (24)

${}^i\boldsymbol{n}_i^J=\sum_m(F_m^{Ti}\boldsymbol{f}_{im}^M)\times{}^i\boldsymbol{r}_{im}$ (25)

In order to calculate the muscular tension, not only the active state q_m, but also the geometrical state such as the length of the contractile element L_m^{CE}, and the contractile velocity $\dot{L}_m^{CE}$ are necessary. However, in this study, these geometrical variables were assumed to be given by those values just before one time step of the calculation, for solving q_m.

The objective function J' is the sum of the reciprocals of the endurance times and is minimized in the optimization process. The constraints are the relations between the muscular tension F_m^T and the active state q_m (Eqs.(10) to (16)), the non-negative condition of muscular tension (Eq.(24)), and the equilibrium of the joint torques ${}^i\boldsymbol{n}_i^J$ and muscular torques (Eq.(25)). The calculation of this optimization was performed independently with respect to each body chain group, i.e., 4 limbs and the trunk. After the calculation of the optimized muscular tensions, the lengths of muscle components were calculated using Eqs.(17) to (20).

The uniqueness of this calculation method of muscular tensions is in the consideration of muscle components and length. The objective function based on the muscle fatigue seems to be suitable for moderate and continuous motions such as walking.

2.6 Calculation of energy consumption

The energy consumed due to body motion can be divided into energy consumed due to muscle activity and energy consumed due to visceral activity. The energy consumed by muscle is divided into three components as follows[16]:

$$E=\sum_m(E_m^M+E_m^S+E_m^W)+E^B, \tag{26}$$

where E is the total energy consumption, E_m^M is the muscle maintenance heat, E_m^S is the muscle shortening heat, E_m^W is the muscle mechanical work, and E^B is the basal metabolic energy for life support.

The muscle maintenance heat (energy consumed in proportion to the muscular tension) is expressed as

$$E_m^M=\int\sum_{n=1}^{3}w_{nm}\varepsilon_n^M k(\dot{\xi}_m)q_{nm}dt, \tag{27}$$

where w_{nm} is the mass of each muscle fiber and ε_n^M is the coefficient of the muscle maintenance heat. The values are identical for all muscles (ε_n^M=26.4, 55.8, 97.5[W/kg]).

The muscle shortening heat (energy consumed in proportion to shortening rate) is expressed as

$$E_m^S=\begin{cases}\int(-\dot{L}_m^{CE})\sum_{n=1}^{3}\varepsilon_n^S\bar{F}_{nm}^{CE}k(\dot{\xi}_m)q_{nm}dt & (\dot{L}_m^{CE}<0)\\ 0 & (\dot{L}_m^{CE}\geq 0),\end{cases} \tag{28}$$

where ε_n^S is the coefficient of the muscle shortening heat. The values are identical for all muscles (ε_n^S= 0.20, 0.35, 0.35[Wsec/m]).

The muscle mechanical work is expressed as

$$E_m^W=\begin{cases}\int(-\dot{L}_m^{CE})F_m^{CE}dt & (\dot{L}_m^{CE}<0)\\ 0 & (\dot{L}_m^{CE}\geq 0).\end{cases} \tag{29}$$

The basal metabolic energy (energy consumed due to visceral activity) is expressed as[17]

$$E^B=\int(0.685\ W+29.8)dt, \tag{30}$$

where W is the body weight [kg].

The maximum force exerted by each muscle fiber $\bar{F}_{nm}^{CE}$ in Eq.(11) and Eq.(28), and the mass of each muscle fiber w_{nm} in Eq.(27) are given by

$$\bar{F}_{nm}^{CE}=\bar{A}_m^M R_{nm}\lambda_n, \tag{31}$$
$$w_{nm}=\bar{A}_m^M R_{nm}\bar{L}_m^M\rho, \tag{32}$$

where R_{nm} is the component ratio of the muscle fiber, λ_n is the maximum muscle force per unit cross-sectional area of each muscle fiber (λ_n=0.4, 0.5, 0.6[N/mm^2]), and ρ is the muscle density (ρ=1050[kg/m^3]).

The length of the muscle fiber $\bar{L}_m^M$ and the length of the tendon $\bar{L}_m^T$ were normalized by the length of the

muscle $\bar{L}_m^{MT}$. Consequently the necessary data for each muscle are reduced to collectable anatomical data such as the physical cross-sectional area $\bar{A}_m^M$, the component ratio of the muscle fiber R_{nm}, the length ratio of the muscle to the muscle-tendon complex $\bar{L}_m^M/\bar{L}_m^{MT}$, pennate angle $\bar{\alpha}_m$, the cross-sectional area of the tendon $\bar{A}_m^T$, and the length ratio of the tendon to the muscle-tendon complex $\bar{L}_m^T/\bar{L}_m^{MT}$. In this study, these parameters were obtained from the literature[9),(10)]. For instance, parameters of typical muscles of the lower extremity are shown in Table 3. These values are kept constant regardless of alteration of the link model.

2.7 Calculation procedure

Figure 3 shows the total calculation flow in this simulation. The rigid link model is constructed by designating the names of segments to be analyzed, and the mechanical properties of each link are adjusted by the stature and weight of the subject. Since all anatomical and physiological parameters are written in the data file, they can be easily customized by a user of this program. The program is written in C language. The calculation performed by a personal computer (AST Research, Power Premium 4/50d, CPU: 80486DX2-50MHz) took about 30 seconds per each posture when we use the model in Fig. 6(a). The most of the calculation time is taken in the optimization process of muscular tensions. A quasi-Newton method was used for the numerical calculation.

Table 3 Examples of parameters of leg muscles

Muscle name	$\bar{A}_m^M$ [mm²]	R_{nm} [%] SO	FO	FG	$\bar{L}_m^M/\bar{L}_m^{MT}$	$\bar{\alpha}_m$ [deg]	$\bar{A}_m^T$ [mm²]	$\bar{L}_m^T/\bar{L}_m^{MT}$
Tibialis anterior	1700	70	10	20	0.208	10	20	0.8
Soleus	18700	75	15	10	0.103	15	17	0.8
Vastus medialis	6700	50	15	35	0.198	25	32	0.2
Biceps femoris, L	2700	65	10	25	0.146	15	20	0.45
Rectus femoris	4300	45	15	40	0.102	15	24	0.4
Iliacus	2300	50	20	30	1.000	0	0	0
Adductor longus	2300	65	15	20	1.000	0	0	0
Gluteus medius	2500	50	20	30	0.850	0	20	0.15
Gluteus maximus	2000	50	20	30	0.900	0	46	0.1

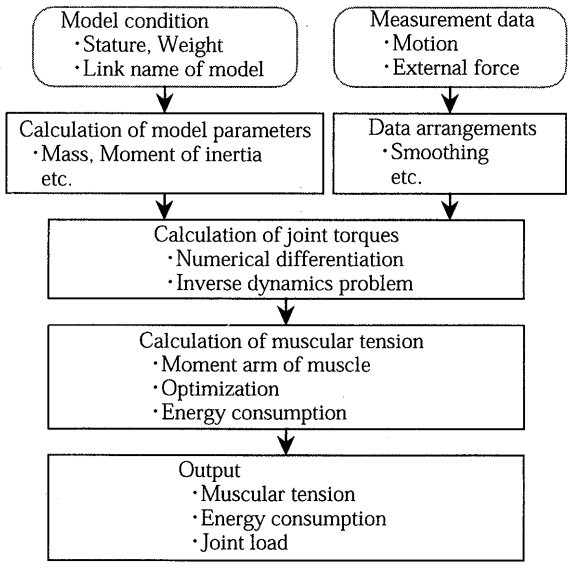

Fig. 3 Calculation flow

3. Evaluation and Examples of the Simulation

Normal walking was analyzed as an example of a simplified link model (8 links and 40 muscles of the one side) and rowing motions were analyzed as an example of a whole-body model (13 links and 31 muscles of the one side). Body motions were assumed symmetry and were measured three-dimensionally with two sets of an opto-electronic camera system (Hamamatsu Photonics, PSD system C3570). External forces were measured using a force plate (Kyowa Dengyo, EP-386) in walking, and a rowing ergometer (Concept II) with foot force sensors fabricated in our laboratory.

3.1 Evaluation of model performance

The estimated tensions in principle muscles during walking are shown in Fig. 4. The model for normal walking consists of 8 body segments (feet, shanks, thighs, pelvis, HAT (head, arm, upper trunk)) and 40 muscles are attached to each leg. In Fig. 4, the dotted lines represent the EMG patterns taken from Inman's report[18]. These lines are traced so that the peak amplitudes coincide with those of the calculated muscular tensions. The agreement of the two changing patterns demonstrates the validity of this method.

The relationship between total energy consumption and walking speed is shown in Fig. 5. Each dot is the calculated energy consumption and the curve is the regression result of the respiration gas analysis performed by Ralston[19]. The two of these are well agreed to each other qualitatively, confirming the

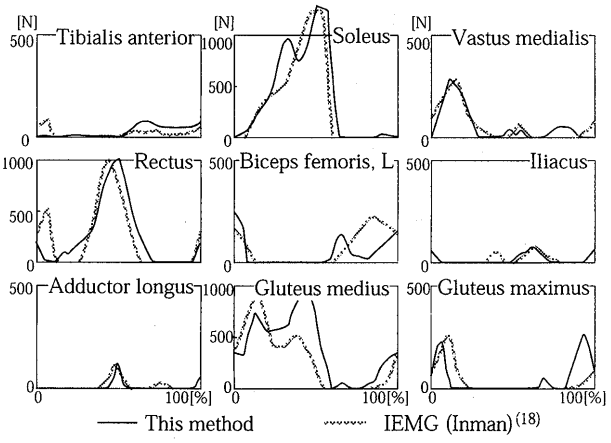

Fig. 4 Muscular tension in walking

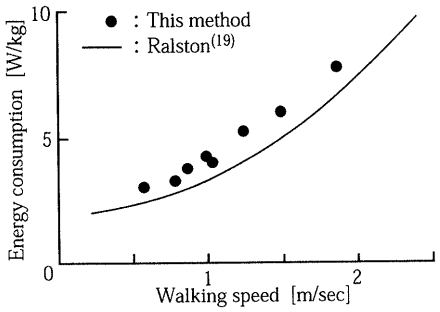

Fig. 5 Relationship between total energy consumption and walking speed

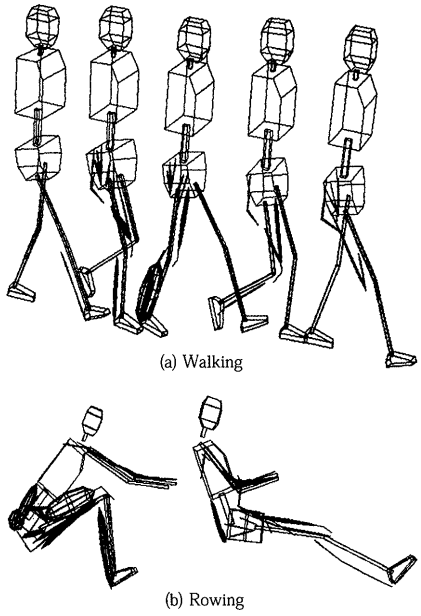

Fig. 6 Three-dimensional stick pictures

adequacy of this calculation.

3.2 Examples of inner load

Muscular tension images for walking and rowing motions are shown as three-dimensional stick pictures in Fig. 6. In this figure, the thickness of each muscle is in proportion to the magnitude of muscular tension. These visualizations of the calculated results facilitate understanding of the complex activities of muscles. In these examples, we can observe easily that the gastrocnemius and soleus in walking, and the quadriceps femoris, gluteus maximus and back muscles in rowing motions exert strong forces.

4. Conclusion

A three-dimensional whole-body musculoskeletal model was developed. By using the model, we can easily obtain the internal loads such as muscular tension, load on bones and joints, and energy consumption for various motions of the human body. Some details of the musculoskeletal model, especially regarding the torso and arm segments, must be improved. More precise anatomical data will be obtained through quantitative analysis of CT (Computed Tomography) and MRI (Magnetic Resonance Imaging).

Acknowledgments

The authors gratefully acknowledge the help of Mr. Motoshi Kaya in the rowing experiment.

References

(1) Winter, D. A., Biomechanics and Motor Control of Human Movement (2nd ed.), (1990), John Wiley & Sons.
(2) Zajac, F. E., Muscle Coordination of Movement: A Perspective, J. Biomech. Vol. 26, Suppl. (1993), p. 109.
(3) Davy, D. T. and Audu, M. L., A Dynamic Optimization Technique for Predicting Muscle Forces in the Swing Phase of Gait, J. Biomech., Vol. 20, No. 2 (1987), p. 187.
(4) Sasada, T., Tsukamono, Y. and Mabuchi, K., Bio-Tribology, (in Japanese), (1988), Sangyotosho.
(5) Chandler, R. F., Clauser, C. E., McConville, J. T., Reynolds, H. M. and Young, J. W., Investigation of Inertial Properties of the Human Body, (1975), U. S. Government Printing Office.
(6) Zatsiorsky, V. and Seluyanov, V., The Mass and Inertia Characteristics of the Main Segments of the Human Body, Biomechanics, Vol. 8 (1983), p. 1152, Human Kinetics Publishers.
(7) Pierrynowski, M. R. and Morrison, J. B., A Physiological Model for the Evaluation of Muscular Forces in Human Locomotion: Theoretical Aspects, Math. Biosci., Vol. 75 (1985), p. 69.
(8) Delp, S. L., Loan, J. P., Hoy, M. G., Zajac, F. E., Topp, E. L. and Rosen, J. M., An Interactive Graphics-Based Model of the Lower Extremity to Study Orthopaedic Surgical Procedures, IEEE Trans. Biomed. Eng., Vol. 37, No. 8 (1990), p. 757.
(9) Winters, J. M. and Woo, S. L., Multiple Muscle Systems, (1990), Springer-Verlag.
(10) McMinn, R. M. H. and Hutchings, R. T., A Color Atlas of Human Anatomy, (1977), Wolfe Medical Publications.
(11) Hatze, H., A Myocybernetic Control Model of Skeletal Muscle, Biol. Cybern., Vol. 25 (1977), p. 103.
(12) Winters, J. M. and Stark, L., Estimated Mechanical Properties of Synergistic Muscles Involved in Movements of a Variety of Human Joints, J. Biomech., Vol. 21, No. 12 (1988), p. 1027.
(13) Dul, J., Johnson, G. E., Shiavi, R. and Townsend, M. A., Muscular Synergism-II. A Minimum-Fatigue Criterion for Load Sharing between Synergistic Muscles, J. Biomech., Vol. 17, No. 9 (1984), p. 675.
(14) Benedict, J. V., Walker, L. B. and Harris, E. H., Stress-Strain Characteristics and Tensile Strength of Unembalmed Human Tendon, J.

Biomech., Vol. 1 (1968), p. 53.
(15) Crowninshield, R. D. and Brand, R. A., A Physiologically Based Criterion of Muscle Force Prediction in Locomotion, J. Biomech., Vol. 14, No. 11 (1981), p. 793.
(16) Hatze, H. and Buys, J. D., Energy-Optimal Controls in the Mammalian Neuromuscular System, Biol. Cybern., Vol. 27 (1977), p. 9.
(17) Yoshimura, N., Iwase, Y. and Kawakami, M., Outline of Medical Physiology, (in Japanese), (1979), Nankoudo.
(18) Inman, V. T., The Pattern of Muscular Activity in the Lower Extremity during Walking, (1953), Univ. California, Ser. II, Tech. Rept., 25.
(19) Ralston, H. J., Energy-Speed Relation and Optimal Speed during Level Walking, Int. Z. Angew. Physiol., Vol. 17 (S), (1958), p. 277.